CHEMICAL ENGINEERING TRANSACTIONS

VOL. 52, 2016

A publication of
AIDIC
The Italian Association
of Chemical Engineering
Online at www.aidic.it/cet

Guest Editors: Petar Sabev Varbanov, Peng-Yen Liew, Jun-Yow Yong, Jiří Jaromír Klemeš, Hon Loong Lam

ISBN 978-88-95608-42-6; **ISSN** 2283-9216

DOI: 10.3303/CET1652050

Hydrogen Production by a Thermally Integrated ATR based Fuel Processor

Antonio Ricca*[a], Vinceinzo Palma[a], Biagio Addeo[a], Gaetano Paolillo[b]

[a]University of Salerno, Department of Industrial Engineering, via Giovanni Paolo II 132, 84084 Fisciano (SA), ITALY
[b]SOL S.p.A. - 20900 Monza (MB) - ITALY
aricca@unisa.it

In the present work, a very compact reaction system thermally integrated for the distributed hydrogen production by natural gas reforming is reported. The system is based on hydrocarbon Auto-Thermal Reforming, followed by a Water-Gas Shift module. A compact heat exchanger was placed between the two catalytic stages, in order to assure an appropriate thermal integration that avoid any other external heat duties. Experimental results demonstrated that the integrated configuration assured a good management of thermal fluxes in the system, in which an effective heat recovery from ATR exhaust gas to reactants was realized. Preliminary tests showed very impressive performances of the system, both by processing methane and natural gas. Despite a quite slow WGS stage, the processor was able to produce up to 10 Nm^3/h of hydrogen, assuring a thermal efficiency higher than traditional systems.

1. Introduction

The importance of research aimed to enable the introduction of hydrogen as a clean fuel can hardly be overstated, and the introduction of the hydrogen economy is a stated policy goal of the UE. Widespread use of hydrogen for fuelling transportation is a key element of a proposed hydrogen economy. The drawbacks of hydrogen use are high carbon emissions intensity when produced from natural gas, capital cost burden, low energy content per unit volume, low performance of fuel cell vehicles compared with gasoline vehicles, production and compression of hydrogen, and the large investment in infrastructure that would be required to fuel vehicles. The lack of infrastructure for hydrogen production and the unsolved hydrogen storage problem are accelerating the development of compact fuel reformers able to produce a hydrogen-rich syngas from hydrocarbons. The aim of a fuel processor is to convert a hydrocarbon in a H_2-rich stream. Typically, it consists in three main steps: a reforming unit, in which syngas is produced by hydrocarbons, a water gas shift unit to convert CO in further H_2, and a preferential oxidation unit, to remove any CO traces from syngas. There are three primary techniques used to produce hydrogen from hydrocarbon fuels: steam reforming (SR), partial oxidation (POX), and auto-thermal reforming (ATR). The choice of the proper reforming chemistry is the starting point to design an effective reforming process.

The ATR (Eq. 1) is a combination of SR and POX, in which hydrocarbon reacts both with steam and oxygen:

$$CH_4 + xO_2 + yH_2O \rightleftarrows aCO + bCO_2 + cCH_4 + dH_2O + eH_2 + fC_{(s)} \tag{1}$$

In earlier literature, ATR may be considered as the sequence of POX and SR: it is a self-sustained catalytic process, in which the exothermicity of hydrocarbon oxidation reaction supplies to the system the heat needed for the SR reaction. As a consequence, the thermal profile along the catalyst is characterized by a huge temperature peak in the first zone, followed by a slow temperature decreasing until the end (Palma et al., 2013). For distributed H_2 production, simple very compact and versatile systems, characterized by fast start-up time and very quick response to feed changes are required. To this goal, the chemical characteristics of ATR reaction, like high reaction rate, and the ability to work without any external heat sources, candidate the ATR of hydrocarbons as one of the most promising selection (Ciambelli et al., 2009).

Please cite this article as: Ricca A., Palma V., Addeo B., Paolillo G., 2016, Hydrogen production by a thermally integrated atr based fuel processor, Chemical Engineering Transactions, 52, 295-300 DOI:10.3303/CET1652050

Since ATR reaction involves three different reactants, both liquid and gaseous, it is very important to obtain proper reactants mixing: a non-uniform mixing of reactants may cause local lack of reagents, with a decrease of yield and selectivity towards desired products, coke formation, and catalyst deactivation. In order to reduce plant size and operating costs, very advantages may be achieved by heat transferring from product stream to feed streams (Chen et al., 2010). To choose and setup the catalytic system results as a fundamental step in the ATR reaction system design. Catalyst selection may greatly affect both the conversion degree and the selectivity of the reaction, so the presence of some actives species rather than others can lead to different reaction products. The ATR process may be considered as the synthesis of SR and POX, therefore the catalyst in one hand must ensure a high selectivity towards these two reactions, on the other hand must inhibit hydrocarbon cracking reactions, that lead to the catalyst deactivation. Several studies have demonstrated that nickel as well as noble metals (Pt, Rh, Ru) supported on Al_2O_3, CeO_2 or ZrO_2 show good activity toward reforming reactions; improvements in stability and selectivity are achieved from bimetallic catalytic systems (Italiano et al., 2016). Great attention must be also devoted to the catalyst structure (e.g. powder, pellets, honeycomb, foams, etc.). Previous studies have demonstrated that high thermal conductivity supports allow a flat thermal profile along catalytic bed, and thus a higher outside temperature of products that leads at higher hydrocarbon conversion (Palma et al., 2015). In this way, metal based honeycomb monoliths and foams are selected as the best supports for ATR catalytic systems. Furthermore, such supports minimize pressure drops along catalytic bed and reduce the risk of hot-spot phenomena that may cause coke formation and thus catalyst deactivation (Xu et al., 2013).

In this work, a catalytic ATR based fuel processor thermally integrated was designed and tested, in order to produce a H2 rich stream by methane or natural gas conversion. The system will be capable to produce up to 10 Nm^3/h of hydrogen by a self-sustained processing, without any external heating supply. The main purpose of the tests was to understand the influence of operative parameters in the system performances.

2. Experimental

Based on a former concept of ATR based reactor (Palma et al., 2013), a fuel processor was designed and realized, able to produce up to 10 Nm^3/h of hydrogen from gaseous hydrocarbons sources. Experimental reactor (Figure 1) was mainly composed by 4 modules: a mixing unit, aimed to ensure a uniform reactants stream; a ATR catalytic unit, devoted to the reforming reactions, in which hydrocarbons should be converted; a heat recovery unit, in which reactants are pre-heated; a WGS catalytic unit, in which carbon monoxide is converted.

The heat exchange module (or heat recovery module) could be identified as the most important component of the reaction system: it is placed between ATR and WGS modules. Its role is to pre-heat reactants by exploiting exhaust products stream sensible heat: in this way, it is possible at the same to obtain overheated steam and air, and to cool products stream up to a temperature consistent to further WGS stage. The module was composed by three heat exchangers, two of which devoted to water vaporization and overheating, and one devoted to the air heating. Each heat exchanger consists in a series of rectangular coils, realized with AISI316 stainless steel tubes (o.d. 1/8”, thickness 0.74 mm), mounted in parallel-way on two manifolds (in and out) (Figure 1(a)).

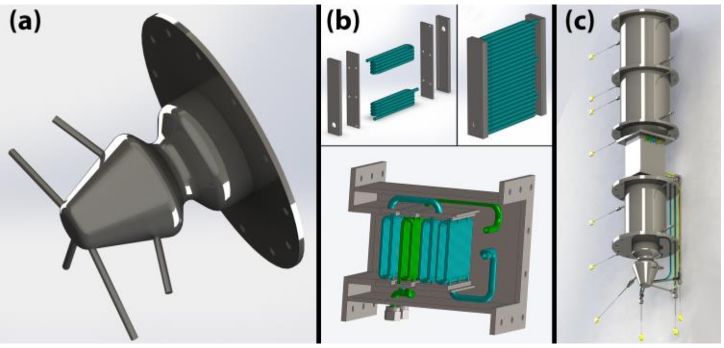

Figure 1: (a) Mixing Module; (b) Views of heat exchangers component; (c) Assembled Fuel Processor

The use of several coils mounted parallel-way at same time increases heat exchange efficiency and reduces pressure drops. The heat exchangers are mounted in a rectangular module, in transversal-way respect to the exhaust gas flux, to create a uniform cross section and thus to maximize the overall heat transfer (Figure 1(c)). It was so created a tube-shell like heat exchangers: the reactants flow in the tube-side, and the exhaust gas flow in the shell-side.

The reaction system was supplied by 3 different streams (air, methane, and steam): the proper reactants mixing could therefore affect the overall system performances. In this aim, the mixing module, realized in stainless steel AISI 316L, was designed to assure a very homogeneous reactants mixture. It appears as three opposite truncated cone (Figure 1(a)): its subsequent expanding and shrinking sections allowed the formation of eddies and whirlpools, realizing a very effective reactants mixing that results in uniform temperature and composition at the inlet of the catalytic module. A spark plug placed at the end of the module allows the system start-up.

Catalytic reactions take place in the two reaction units: the ATR module and the WGS module. Both modules were characterized by a cylindrical shape, in order to effectively host commercial monolithic catalysts.

The external size of the module was D 140 x H 216 mm, while the wall thickness was 5 mm. Inside ATR module, a commercial noble metal based catalyst (supplied by Johnson Matthey) is placed; the catalyst is a cylindrical honeycomb monolith (400 CPSI - WT 6.5 mil), with diameter 3.66” (around 93 mm) and length 6” (around 152 mm), corresponding to a total volume of about 1,000 cm^3. The monolith was wrapped in a layer of insulating and inert material, so avoiding by-pass phenomena of catalytic area, and improving the thermal insulation of the catalytic zone, obtaining a quasi-adiabatic reaction.

The WGS unit, placed downstream the heat recovery module, was constituted by two cylindrical tubes, each sized D 170 x H 216 mm and realized in stainless steel AISI 316 with a wall thickness of 5 mm. In the module a commercial 5 mm pellets catalyst (Katalco$_{JM}$ 71-5M) was loaded, up to achieve a total volume of 7,500 cm^3.

A couple of thermocouples and sampling lines were placed in correspondence of the inner and outer section of the catalytic volume, in order to assure an accurate processes monitoring along the reaction system.

All modules are fixed between them by means of special flanges (Figure (c)) that assured an easy management and a quick system disassemble; to avoid gas leakage, graphite gaskets were used between flanges. The system is wrapped in layers of insulating foam, in order to reduce heat loss in the surround.

The experimental tests were carried out in conditions very close to practical utilization of the prototype. Therefore, compressed atmospheric air and industrial service water was used as reactants. Moreover, experimental tests were carried out both on pure methane (99.5% purity, provided by SOL S.p.a.) and industrial natural gas (provided by SNAM S.p.a. network distribution). All reactants were delivered to the system by thermal mass flow controllers provided by Bronkhorst. Experimental tests were performed by evaluating both the effect of feed ratios and gas rate: O_2/fuel ratio ranged between 0.55 and 0.65, while H_2O/fuel ratio ranged between 0.6 and 1.00; the reactants rate (evaluated in terms of gas hourly space velocity (GHSV) = $Q_{tot}/V_{CAT\text{-}ATR}$) ranged between 15,000 to 22,500 h^{-1}.

Reaction progress in each unit was assured by means of a series of sampling lines, managed by manual valves, that, after condensing steam by a cooling bath, were connected to an ABB multi-gas analyser (IR sensor for CO, CO_2 and CH_4, TCD sensor for H_2, paramagnetic sensor for O_2) for the volumetric composition measurement.

3. Results and discussion

Preliminary tests on integrated system were carried out by feeding methane to the system; the gas hourly space velocity was fixed to 15,000 h^{-1}, while the O_2/CH_4 ratio to 0.65; the effect was evaluated, by varying the steam-to-carbon ratio between 0.6 and 0.75. Experimental results were summarized in Figure 2 and Table 1.

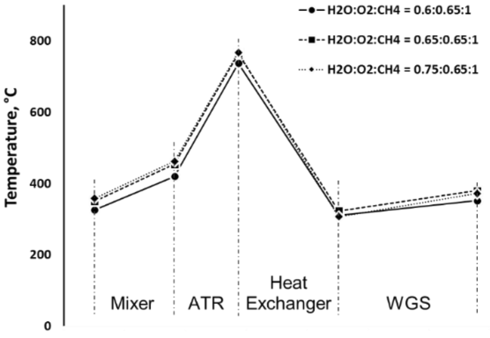

Figure 2: Thermal profiles along the system during the methane processing (GHSV = 15,000 h^{-1})

By feeding reactants at room temperature, heat recovery module was able to effectively transfer heat from exhaust gases out-coming from ATR module to the reactants, resulting in a stream temperature ranging from 325 °C and 360 °C. The ATR module generated a huge temperature increasing, since exhaust stream temperature was around 750 °C for all investigated conditions. In the heat exchange module, process stream was cooled up to about 300 °C before entering in the WGS module, in which the weakly exothermic process resulted in a sensible temperature increasing.

Table 1: Gas composition and unit conversions during the methane processing (GHSV = 15,000 h^{-1})

1	ATR							WGS							
	H_2O/C	O_2/C	H_2 *%vol*	CH_4 *%vol*	CO *%vol*	CO_2 *%vol*	Conv. CH_4 %	H_2O/CO	T_{IN} °C	T_{OUT} °C	H_2 *%vol*	CH_4 *%vol*	CO *%vol*	CO_2 *%vol*	Conv. CO %
CASE 1	0.60	0.65	**37.1**	**0.6**	**14.3**	**4.9**	**99.0** *(98.9)*	0.70	311	352	**40.3**	**0.4**	**6.5**	**11.0**	**52.1** (56.7)
CASE 2	0.65	0.65	**37.**	**0.3**	**14.3**	**4.8**	**99.5** *(99.4)*	0.70	323	380	**41.2**	**0.3**	**6.5**	**10.9**	**51.8** (53.0)
CASE 3	0.75	0.65	**37.7**	**0.3**	**13.9**	**5.3**	**99.5** *(99.6)*	0.85	307	372	**41.5**	**0.3**	**6.2**	**11.1**	**52.5** (58.3)

System performances, summarized Table 1, evidenced the overall appreciable behaviour of the integrated system. Globally, the system was able to produce a gas stream with more than 40 % of hydrogen in the investigated operating conditions. About the single catalytic units, ATR module showed excellent performances, since a clear overlap to thermodynamic equilibrium values was recorded. As a consequence, a methane conversion up to 99.5 % was observed, so reducing hydrocarbon content below 0.3 % in the exhaust stream. A weak increasing of CO shift (in the ATR module) was recorded by increasing fed water to the system, since CO decreases from 14.3 % to 13.9 %, with a corresponding increasing of CO_2.

A different situation was observed in the Water-Gas Shift module, in which in one hand a farer approach to thermodynamic equilibrium value was recorded, in the other hand very low CO conversion was achieved in the 3 investigated operating conditions. It was remarkable that low steam-to-CO ratio were evaluated at the inlet of WGS unit, mainly due to the low steam-to-carbon ratio delivered to the system. Such condition led to severe thermodynamic constrictions, since CO conversion lower than 60 % was thermodynamically expected, thus effecting the overall system performances. Moreover, it is remarkable that WGS catalyst was characterized by very low kinetics, since the system appeared not able to reach thermodynamic equilibrium despite the relatively low gas rate / catalytic volume ratio (in the WGS, a GHSV value below 3,500 h^{-1} is evaluated). It is also noticeable that higher H_2O/CO ratio seems to improve CO conversion, but did not affect the approach to thermodynamic equilibrium. On the other hand, a clear dependence between the gas temperature at the inlet of WGS catalyst and the approach to thermodynamic equilibrium may be observed, since the high temperature recorded in the Case 2 led to a CO conversion very close to thermodynamic prediction.

Experimental tests were also carried out by feeding natural gas to the system; in a first run, the gas hourly space velocity was fixed to 15,000 h^{-1}, while feed ratios effect was investigated by varying the O_2/NG ratio between 0.55 and 0.60 and the H_2O/NG ratio between 0.70 and 1.00. Finally, the effect of feed stream rate was investigated: the feed ratio was fixed in $H_2O:O_2:NG$ = 0.8:0.6:1, while GHSV was varied between 15,000 and 22,500 h^{-1}. Results were summarized in Figure 3, Table 2 and 3.

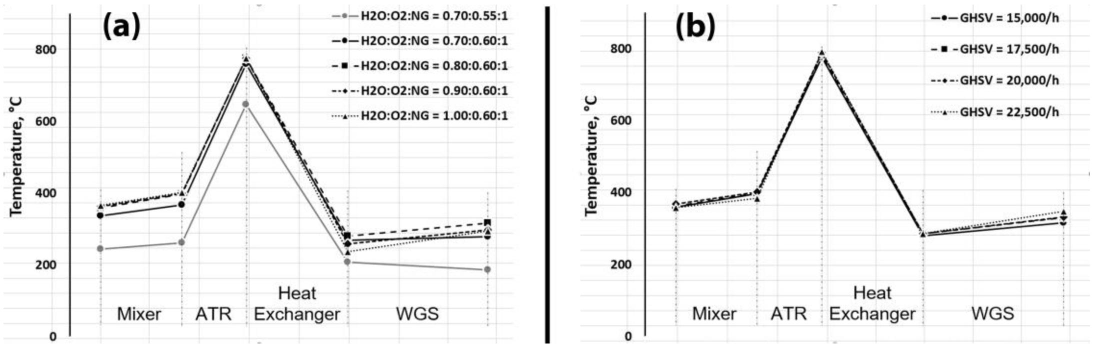

Figure 3: Thermal profiles dependence on feed ratios (GHSV = 15,000 h^{-1}) (a) and feed rate ($H_2O:O_2:NG$ = 0.80:0.60:1) (b)

Temperature profile diagram evidenced that oxygen content delivered to the system dramatically affected the temperature of the system: by increasing O_2/NG from 0.55 to 0.60, temperature profile recorded an overall mean raising of more than 90 °C. On the other hand, steam-to-natural gas ratio appeared to not have relevant influence on the overall temperature profiles, similarly to what observed in the case of methane processing. It is interesting to focus on influence of H_2O/NG ratio on process stream temperature in the mixer and at the end of heat exchanger: by increasing fed water, higher temperature was recorded in the mixer, and lower temperature was achieved out of heat recovery module. Such behaviour may be devoted to the role of water in the heat recovery unit, that acted as an excellent thermal vector, thus effectively subtracted heat from ATR exhaust steam and then increasing reactants temperature. On the other hand, water-richer feed ratios required higher heat duty for a proper reactants pre-heating, mainly due to the water vaporization, therefore excessive cooling of process stream may occur, resulting in a temperature too low for WGS stage.

Table 2: Gas composition and unit conversions during the methane processing (GHSV = 15,000 h^{-1})

1	ATR							WGS							
	H_2O/ NG	O_2/ NG	H_2 $\%_{vol}$	CH_4 $\%_{vol}$	CO $\%_{vol}$	CO_2 $\%_{vol}$	Fuel Conv. %	H_2O/CO	T_{IN} °C	T_{OUT} °C	H_2 $\%_{vol}$	CH_4 $\%_{vol}$	CO $\%_{vol}$	CO_2 $\%_{vol}$	Conv. CO %
CASE 1	0.70	0.55	**37.7**	**3.9**	**10.2**	**7.8**	**83.9** *(88.3)*	1.67	207	186	**38.2**	**4.0**	**7.4**	**10.7**	**17.9** *(96.5)*
CASE 2	0.70	0.60	**35.3**	**1.7**	**15.2**	**4.7**	**91.5** *(99.1)*	0.78	268	278	**39.5**	**1.7**	**9.1**	**9.9**	**39.7** *(64.4)*
CASE 3	0.80	0.60	**35.9**	**1.6**	**14.8**	**5.2**	**95.0** *(99.5)*	0.85	280	316	**41.1**	**1.0**	**5.9**	**12.0**	**58.0** *(61.8)*
CASE 4	0.90	0.60	**35.9**	**1.8**	**14.3**	**5.3**	**94.2** *(99.6)*	1.17	258	297	**41.4**	**1.2**	**5.5**	**12.3**	**59.0** *(77.7)*
CASE 5	1.00	0.60	**36.0**	**1.8**	**13.9**	**5.6**	**94.2** *(99.6)*	1.30	237	294	**41.2**	**1.2**	**5.4**	**12.4**	**58.0** *(81.3)*

The gas composition analysis summarized in Table 2 Table 2: Gas composition and unit conversions during the methane processing (GHSV = 15,000 h-1)evidenced that by feeding natural gas instead of methane, a clear worsening in approach to thermodynamic values was achieved in ATR module; such unwanted result seems to not depend on oxygen nor water amounts delivered to the system, suggesting to be devoted to a partial catalyst inactivation due to impurities present in the fuel stream. It is anyway evident that by increasing fed air to the system, the conversion of fuel increased, according the thermodynamic predictions, mainly due to the resulted higher temperature of the ATR unit. Raising steam content, an initial ATR module enhancement could be observed (from Case 2 to Case 3), resulting in a fuel conversion closer to thermodynamic equilibrium prediction. Further steam increasing did not lead to any improvements in terms of conversion, while a weak decreasing of CO content could be reported.

The WGS unit registered similar behaviour with respect to methane processing, since CO conversion appeared quite far from thermodynamic equilibrium. In the Case 1, despite the high Steam-to-CO content, very low activity of WGS stage was recorded, mainly due to the low temperature of the catalyst. A better approach to equilibrium prediction was observed for the Case 3, while further increasing of fed water resulted in a divergence between thermodynamic and experimental conversion values. Therefore, WGS catalytic system suffered not only the lack of water in several conditions, but also the low temperature of the stage, that dramatically affected the catalyst kinetics.

By analysing GHSV effect, quite different T profiles (Figure 3(b)) were achieved in the mixer and in the WGS modules: such behaviours may be ascribed to an improved adiabaticity of the system at higher flux rates. In particular, in the WGS module, in which an exothermic process took place, the more pronounced temperature slope, achieved at the highest gas rate, evidenced a lower heat dispersion fraction of the system, that in turn promotes higher adiabatic temperature. The lower temperature at the inlet of the ATR achieved at the highest GHSV may suggest a less evident radiative effect of the ATR catalyst on the temperature sensor.

Table 3 Gas composition and unit conversions during the methane processing (H_2O:O_2:NG = 0.80:0.60:1)

1	ATR						WGS							
	GHSV h^{-1}	H_2 $\%_{vol}$	CH_4 $\%_{vol}$	CO $\%_{vol}$	CO_2 $\%_{vol}$	Fuel Conv. %	H_2O/CO	T_{IN} °C	T_{OUT} °C	H_2 $\%_{vol}$	CH_4 $\%_{vol}$	CO $\%_{vol}$	CO_2 $\%_{vol}$	Conv. CO %
CASE 3	15,000	**35.9**	**1.6**	**14.8**	**5.2**	**95.0** *(99.5)*	0.85	280	316	**41.1**	**1.0**	**5.9**	**12.0**	**58.0** *(61.8)*
CASE 6	17,500	**35.7**	**1.7**	**14.9**	**4.9**	**94.2** *(99.6)*	0.97	285	330	**40.3**	**1.2**	**7.0**	**11.3**	**48.4** *(65.4)*
CASE 7	20,000	**35.3**	**1.9**	**15.1**	**4.8**	**94.1** *(99.6)*	0.96	285	332	**40.5**	**1.2**	**7.9**	**10.5**	**46.2** *(64.9)*
CASE 8	22,500	**34.8**	**2.2**	**15.1**	**4.7**	**93.8** *(99.7)*	1.03	286	348	**40.7**	**1.3**	**7.1**	**11.1**	**50.6** *(65.2)*

The analysis of composition after catalytic units revealed that increasing of reactants rate reduces conversion in the reactions modules. Lower contact times resulted in a divergence between experimental and thermodynamic conversion values, thus remarking the heavy kinetic limitation of the WGS catalyst in the selected operating conditions.

Finally, overall system performances, in terms of produced hydrogen and thermal efficiency, were summarized in Figure 4. As a main result, the system demonstrated to be able to produce up to 10 Nm^3/h of hydrogen by natural gas processing. The hydrogen production seems to have a quasi-linear dependence on GHSV (and then on reactants rate), thus higher production could be expected. It is also evidenced that by increasing gas rate, a sensible reduction in thermal efficiency occurs, ascribable to the difficulties in the WGS module.

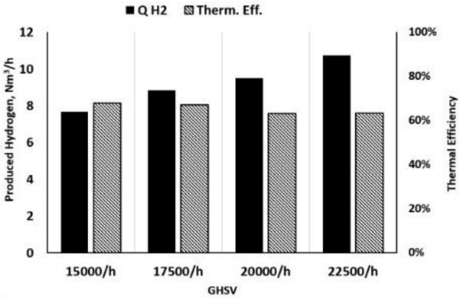

Figure 4: Hydrogen production and thermal efficiency of the system during the methane processing (H_2O:O_2:NG = 0.80:0.60:1)

4. Conclusions

An ATR-based fuel processor thermally integrated was designed, for hydrogen production by methane or natural gas. Preliminary tests evidenced the promising performances of the system, able to self-sustain the hosted processes without external heat sources. Not adequate performances were recorded in the WGS unit, that seems to suffer the severe operating conditions, effecting both system kinetics and thermodynamic limitations. Catalyst formulation requires a too high activation temperature not easy to reach due to the system thermal integration, that also restrains the system in terms of steam-to-carbon monoxide ratio. If in one hand a more appropriate formulation for the WGS catalyst appeared mandatory, characterized by lower activation energy and higher kinetics, in the other hand the WGS module performances should be clearly improved by increasing H_2O/CO feed ratio (by feeding more steam directly to the WGS module). It is reasonable to exploit sensible heat of exhaust gas downstream the WGS unit for reactants pre-heating, so in one hand reducing heat recovery between ATR and WGS stages thus resulting in a higher temperature at the inlet of the CO-shift catalyst, in the other hand increasing steam generation to fed in the catalytic stages.

Anyway, despite the low CO conversion, the system was able to produce up to 10 Nm^3/h of hydrogen, assuring a thermal efficiency of 68 % by natural gas processing; such value may be easily increased up to 71 % by WGS stage optimization (more active catalyst, increased catalytic volume). Finally, it is worth to remark that achieved thermal efficiency is significantly higher than reported efficiency (65 %) of conventional distributed hydrogen production plants.

References

Palma V., Ricca A., Ciambelli P., 2013, Performances analysis of a compact kW-scale ATR reactor for distributed H_2 production. Clean Technologies and Environmental Policy, 15(1), 63-71.

Ciambelli P., Palma V., Palo E., Iaquaniello G., 2009, Natural Gas Autothermal Reforming: an Effective Option for a Sustainable Distributed Production of Hydrogen. In: Barbaro P., Bianchini C. (Eds.), Catalysis for Sustainable Energy Production. Wiley-VCH Verlag GmbH & Co. KGaA, Weinheim, Germany. doi: 10.1002/9783527625413.ch9.

Chen W.-H., Lin M.-R., Lu J.-J., Chao Y., Leu T.-S., 2010, Thermodynamic analysis of hydrogen production from methane via autothermal reforming and partial oxidation followed by water gas shift reaction. International Journal of Hydrogen Energy, 35, 11787-11797.

Italiano C., Balzarotti R., Vita A., Latorrata S., Fabiano C., Pino L., Cristiani C., 2016, Preparation of structured catalysts with Ni and Ni–Rh/CeO_2 catalytic layers for syngas production by biogas reforming processes. Catalysis Today. 273, 3-11.

Palma V., Ruocco C., Castaldo F., Ricca A., Boettge D., 2015. Ethanol steam reforming over bimetallic coated ceramic foams: Effect of reactor configuration and catalytic support. International Journal of Hydrogen Energy, 40, 12650-12662.

Xu X., Li P., Shen Y., 2013, Small-scale reforming of diesel and jet fuels to make hydrogen and syngas for fuel cells: A review. Applied Energy, 108, 202-217.

Palma V., Ricca A., Ciambelli P., 2013, Fuel cell feed system based on H_2 production by a compact multi-fuel catalytic ATR reactor. International Journal of Hydrogen Energy, 38, 406-416.